



Study of the resistance behavior of anatase and rutile thick films towards carbon monoxide and oxygen at high temperatures and possibilities for sensing applications

Xiangoan Li, Ramamoorthy Ramasamy, Prabir K. Dutta *

Department of Chemistry, The Ohio State University, 120 W 18th Avenue, Columbus, OH 43210, United States

ARTICLE INFO

Article history:

Received 12 June 2009

Received in revised form 31 August 2009

Accepted 14 September 2009

Available online 22 September 2009

Keywords:

TiO₂

p–n transition

High temperature CO sensor

ABSTRACT

The resistance changes of thick films of titania were examined in the presence of CO at elevated temperatures ranging from 500 to 1000 °C. Three materials were examined, commercial samples of anatase and rutile and a Cr³⁺-doped rutile prepared in the laboratory. The anatase film exhibited a n-type response to both oxygen and CO in the tested O₂ range of 2–21% and CO from 10 to 2000 ppm at 600 °C, with the response disappearing beyond 700 °C. On the other hand, the rutile films showed an entirely different electrical behavior. Until 1000 °C, p-type response was observed to oxygen concentrations from 2 to 21%. With CO concentrations up to 2000 ppm, p-type behavior was observed in 2–21% oxygen concentrations between 600 and 700 °C. However, when the temperature was above 750 °C, an n-type behavior to CO with concentrations ranging from 200 to 2000 ppm was observed, and response was observed until 850 °C. A coating of colloidal platinum on the rutile film induced a transition of the response of the thick film from p to n-type to both oxygen and CO at 600 °C. With the Cr-rutile sample, p-type behavior was observed for both CO and O₂. The possible mechanisms for the observed p–n transition of the two rutile films are discussed. Strategies for developing CO sensors for high temperature applications based on the above observations are formulated.

© 2009 Elsevier B.V. All rights reserved.

1. Introduction

Titanium dioxide (titania, TiO₂) is used in various gas sensing and catalysis applications. Low temperature synthesis methods usually lead to anatase, with anatase undergoing an irreversible transformation to the more stable rutile phase in the temperature range of 500–1000 °C (controlled by crystallite size), with accompanying grain growth [1]. The electrical properties of titania are influenced by deviation from stoichiometry due to interaction between the oxide surface and surrounding atmosphere and presence of impurity ions. Changes in the oxygen stoichiometry influence the bulk electronic properties, whereas, the presence of impurities can influence both the bulk and the surface properties, depending upon the location of the impurities. Electrical conductivity changes as a function of oxygen non-stoichiometry has been extensively studied and supported by various defect chemistry models [2–6]. The electrical properties of undoped TiO₂ at elevated temperatures depends on pO₂ with n-type conduction at low pO₂ and p-type behavior at high pO₂, the transition point depending on temperature [2–6]. Titania doped with donor impurities such

as Nb⁵⁺ behave as a n-type semiconductor, whereas, with acceptor impurities such as Al³⁺, Fe³⁺, Cr³⁺ the behavior is that of a p-type semiconductor [7,8].

Chemisorption of oxygen on semiconducting oxide surfaces result in formation of O_n^{m-} surface species, the exact form depending on the temperature. Upon oxygen chemisorption on an n-type oxide semiconductor, the electrical resistance across the interface increases. Reducing gases like CO, H₂ can react with the chemisorbed oxygen resulting in a decrease of the resistance, and is the basis for using semiconducting metal oxides, such as TiO₂ as gas sensors. In the case of a p-type oxide semiconductor, the opposite effects in electrical conduction are observed. The change of conduction behavior from n-type to p-type and vice versa has been observed in titania [9], BaTiO₃ [10], SrTiO₃ [11] and α-Fe₂O₃ [12] by varying temperature and impurity doping and gas concentrations.

Within the temperature range of 200–400 °C, the cause of p–n transition observed with transition metal oxides has been attributed to an inversion layer formed on the conduction surface due to oxygen adsorption [12,13]. Based on investigations of the p–n transition of CdS and α-SnWO₄, Solis et al. [14] proposed that reducing gas, e.g. CO can function as surface acceptor leading to the switch of the conduction behavior. Similar mechanism was also proposed by Birkefeld et al. [15] to interpret the sensing behav-

* Corresponding author.

E-mail address: dutta.1@osu.edu (P.K. Dutta).

ior of TiO₂ to reducing gases in N₂ background. At temperatures of 700–800 °C, the surface lattice oxygen of Ga₂O₃ has also been proposed to be involved in the resistance change with reducing gases [16].

There is an increasing demand of high temperature gas sensors with fast response, high sensitivity, reliability and low cost for applications in harsh industrial environments in heat treating, metal processing and casting, automobile and power industries [17–21]. Semiconductor-type chemical gas sensors using transition metal oxides such as SnO₂, Ga₂O₃ and TiO₂ have shown promise for such applications. However, the extensively investigated SnO₂-based sensor functions at temperatures up to 400 °C [22]. Ga₂O₃ has been recently studied for high temperature reducing gas sensors and indicated good sensitivity to methane up to 800 °C [23–26]. Our research group has focused on exploration of TiO₂ for sensing of CO at temperatures around 600 °C [9,27–30]. The sensor using doped anatase showed good sensitivity and selectivity to CO at 600 °C. However, once above 700 °C, the sensitivity of sensor diminished rapidly [29].

In this study, we focus on electrical properties of commercial anatase and rutile thick films, as well as a Cr-doped rutile film. Resistance changes of such films in the presence of CO and O₂ has been studied at 600–1000 °C. Addition of Pt colloids to the rutile films alters their electrical properties. These results provide strategies for fabricating high temperature CO sensors.

2. Experimental

2.1. Materials preparation and characterization

The commercial anatase and rutile titania powder (99.9% Aldrich) were used as the starting material for fabrication of both anatase and rutile thick films, respectively. The 0.5 wt.% Cr-doped TiO₂ powders were prepared by mixing Cr(NO₃)₃·9H₂O (Aldrich) with the rutile TiO₂ powders with a subsequent calcination at 1020 °C for 24 h.

The as-purchased anatase and rutile were calcined at 800 and 1020 °C, respectively, prior to characterization. X-ray diffraction (XRD) patterns were collected on a Rigaku Geigerflex diffractometer using Ni-filtered Cu K α radiation at 40 kV and 25 mA between 2 θ of 20 and 80° at a scanning speed of 12° min⁻¹. High-resolution X-ray photoelectron spectroscopy (XPS) studies were performed with a Kratos AXIS Ultra X-ray photoelectron spectrometer. An Al source was used for all measurements. Experiments were performed at a resolution of 0.02 eV with a pass energy of 5 eV. Charge balancing was used to eliminate charging of the sample during measurement.

2.2. Thick film fabrication

The as-received commercial titania powders and the synthesized Cr-doped TiO₂ powders were mixed with solvent (5V-507 Heraeus) and glue (V-801 Heraeus) to make a paste which was then painted on the alumina substrate pre-printed with the interdigitated Pt electrodes. The anatase thick film was annealed at 800 °C whereas the rutile and Cr-doped TiO₂ thick films were heated at 1020 °C for 2 h. For preparation of the rutile film coated with Pt, platinum colloids prepared by using dipotassium tetrachloroplatinate and polyvinyl alcohol was used [31]. The platinum colloid-PVA dispersion was added drop-wise onto the top surface of the rutile thick films by using a syringe followed by heat treatment at 650 °C for 2 h. Surface morphology of the rutile thick films before and after platinum coating was examined using scanning electron microscopy (SEM: Phillips XL 30 ESEM FEG).

2.3. Electrical measurements

The thick films were tested in an apparatus as described previously [27–31]. Prior to starting the electrical measurement, films were kept at the testing temperature for about 2 h. Gas concentrations of 20–2000 ppm CO were tested. Additionally, measurements of the dependence of the resistance on pO₂ were also conducted at temperatures from 600 to 1000 °C. The films were placed in a quartz cylinder housed at the center of a tube furnace and attached via platinum leads to a Hewlett-Packard HP34970A multiplexer. The multiplexer was operated in high internal impedance mode (~100 M Ω). The temperature was assumed as the set point of the furnace. The gas flow rate was kept constant at 100 standard cubic centimetres per minute. The magnitude of the resistance change was calculated as $S = R/R_0$, where R is the resistance of the film in the CO gas mixture and R_0 in the background gas mixtures of O₂ and N₂ with different oxygen concentrations at 10, 5 or 2% in volume.

3. Results

3.1. Synthesis and characterization

Anatase and rutile forms of titania, obtained from commercial sources are the main focus of this study. These commercial powders were used to print thick films on interdigitated Pt electrodes. The thermal treatment for the anatase sample was done at 800 °C and for rutile at 1020 °C. In addition, a sample prepared by heating a 0.5 wt.% chromium impregnated rutile to 1020 °C was also examined. Fig. 1 compares the power diffraction of the three samples, indicating that with Cr³⁺, rutile remains as the primary phase [32]. Fig. 2 shows the XPS data in the Ti 2p and O 1s region for the anatase and the rutile sample. For the Ti 2p peak, there are no differences between the two samples (Fig. 2a). The O 1s region however, shows differences and these data are shown in Fig. 2b and c for anatase and rutile, respectively, along with the fits. These peaks were fit to three species, with binding energies of 530.5, 531.5 and 533.8 eV [33,34]. In the case of rutile, the intensity of the 533.8 eV peak was negligible.

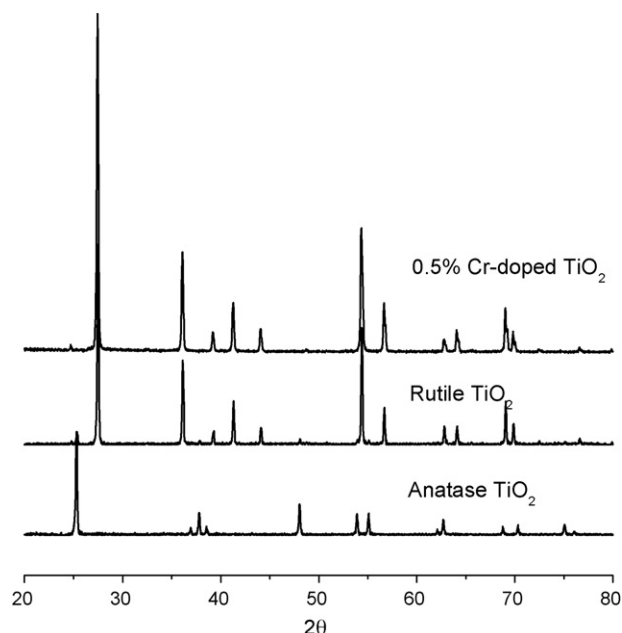


Fig. 1. XRD patterns of anatase, rutile and 0.5% Cr-doped TiO₂.

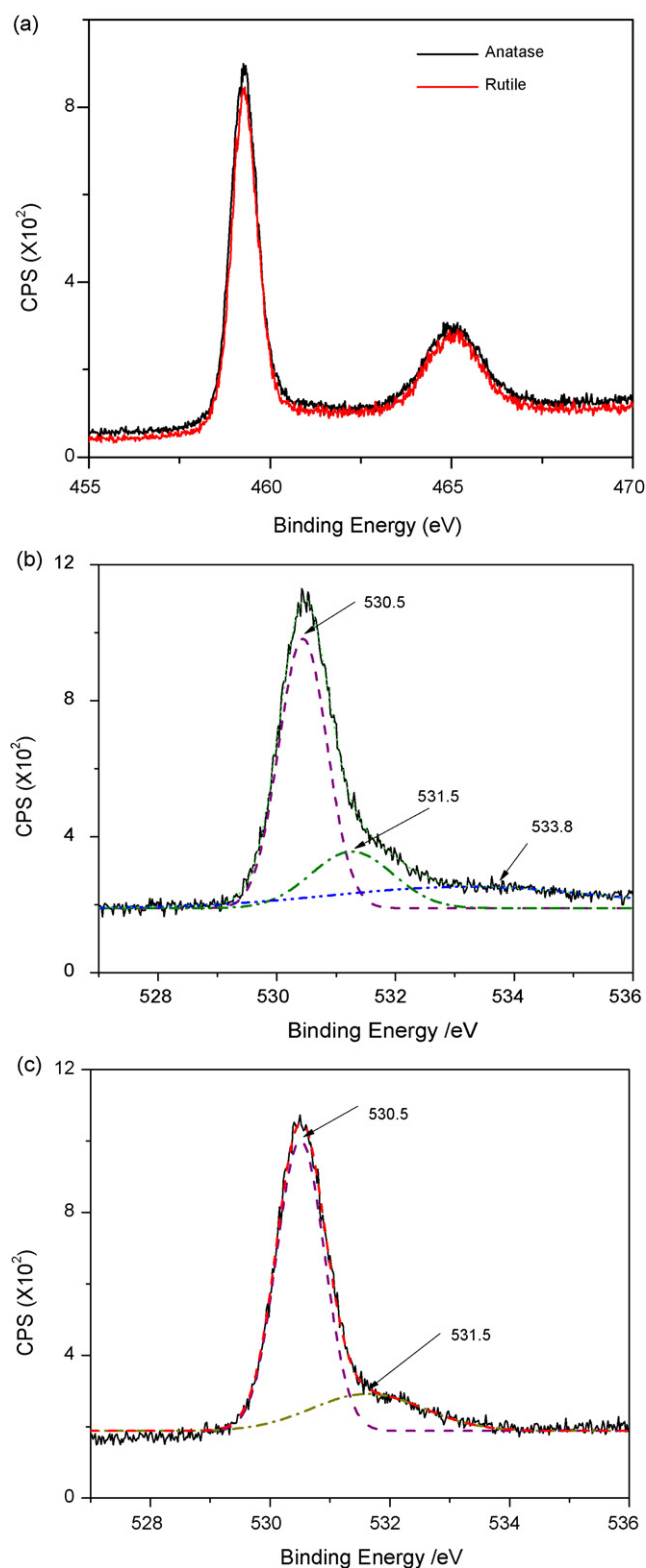


Fig. 2. XPS spectra of anatase calcined at 800 °C and rutile calcined at 1020 °C in the regions of (a) Ti2p; (b) O 1s in anatase and (c) O 1s in rutile.

3.2. Resistance changes with O₂ and CO

3.2.1. Anatase

Fig. 3a shows the change in resistance of an anatase film with O₂ concentration varying from 2 to 10% (balance N₂) and CO varying from 25 to 180 ppm (background 5% and 10% O₂) at 600 °C.

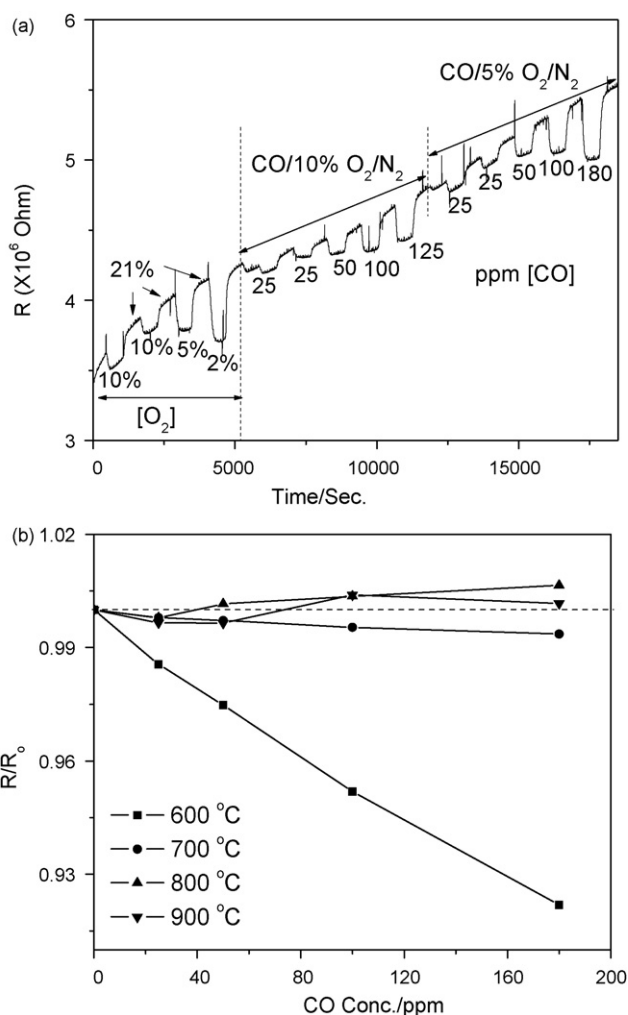


Fig. 3. (a) Response of anatase film to O₂ and CO at 600 °C and (b) sensitivity change of the film (R = resistance of film, R_0 = resistance in background gas) as a function of temperature.

The increase of resistance with increasing O₂ concentration and decrease of resistance with increasing concentration of CO is indicative of n-type behavior. The baseline showed a drift towards higher resistance, but for the purposes of this study, is not relevant. The resistance of the film to CO (R) can be normalized relative to the background resistance (R_0) for any particular CO concentration. Fig. 3b shows the change in response of the anatase film to CO with temperature in a background of 5% O₂/N₂. Above 700 °C, presence of 25 to 180 ppm CO has minimal effect on the resistance of the anatase film. Similar results were observed for CO concentrations upto 1000 ppm.

3.2.2. Rutile

Fig. 4 shows the change in resistance of the rutile film at 700 °C upon exposure to O₂ and CO. A resistance increase is observed with increasing CO concentration, whereas a resistance decrease is observed with increasing O₂ concentration, and suggests that the material is exhibiting p-type behavior. Fig. 5a shows the response to 20–180 ppm CO as a function of temperature in a background of 5% O₂. The response does decrease with temperature, but at 745 °C, there is a crossover from p to n-type behavior at CO concentration exceeding 100 ppm. Fig. 5b focuses on resistance changes at 745 °C and shows that the crossover from p to n-type behavior also depends on O₂ concentration, with higher concentrations of CO necessary to make the switch at higher oxygen concen-

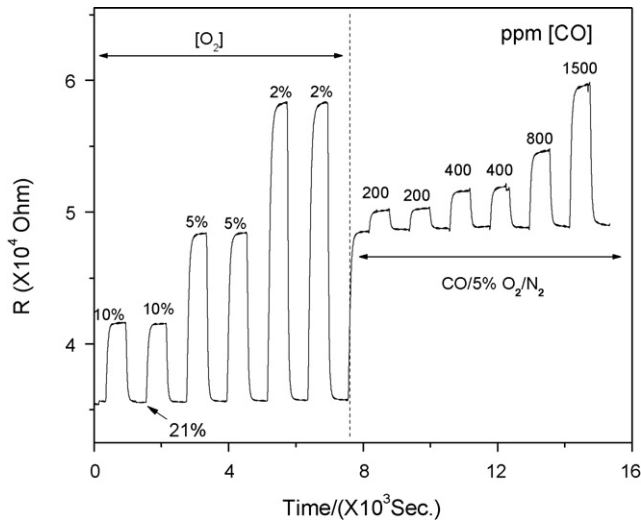


Fig. 4. Response of rutile film calcined at 1020 °C to oxygen and CO at 700 °C.

trations. Fig. 6a shows the behavior of the rutile film at 800 °C, with O₂ (21–2%) exhibiting p-type behavior, but the CO concentration between 200 and 1800 ppm exhibiting n-type behavior under different oxygen backgrounds (2–10%). Fig. 6b shows that the response to CO disappears above 850 °C (data for 5% oxygen,

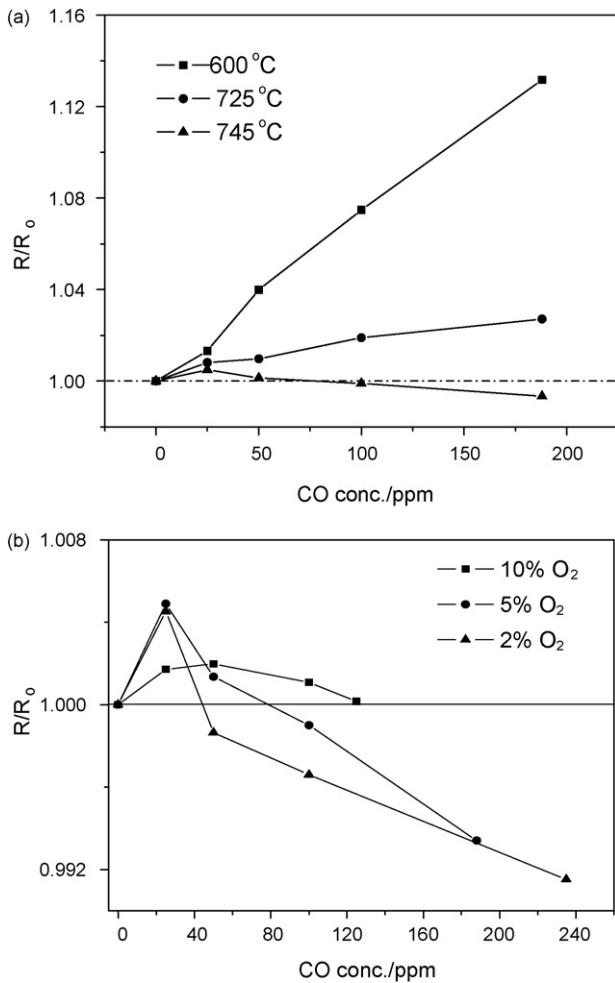


Fig. 5. (a) Sensitivity of the rutile film to CO in 5%O₂ background at temperatures of 600 °C, 725 °C and 745 °C and (b) variation of the sensitivity of the film to CO with the different oxygen concentration backgrounds at 745 °C.

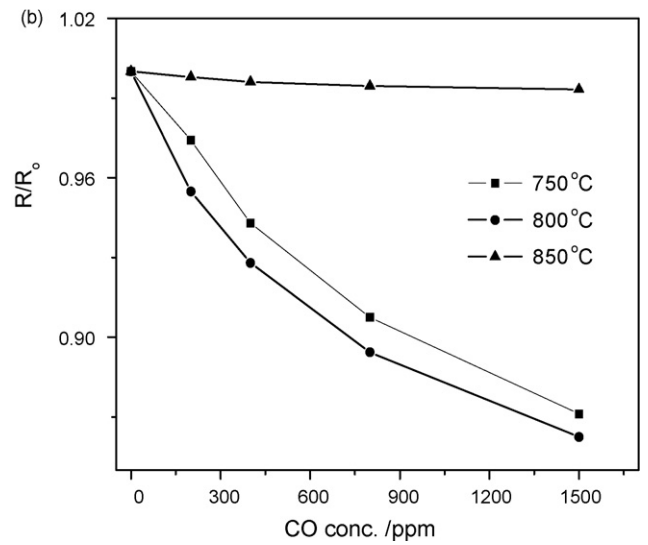
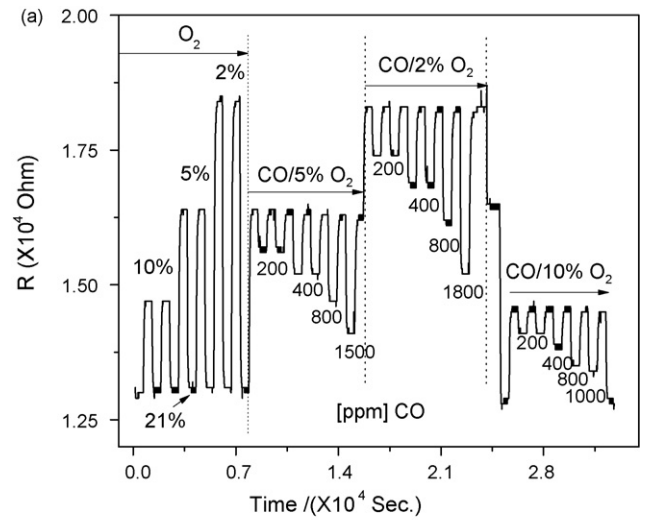


Fig. 6. (a) Response curve of the rutile film calcined at 1020 °C to oxygen and CO at 800 °C and (b) sensitivity of the film to CO in 5%O₂/N₂ background as a function of testing temperatures.

but similar behavior also at 2% and 10% oxygen). Fig. 7 shows that the p-type behavior towards oxygen switches at 1000 °C.

Fig. 8 shows the resistance changes of a rutile film which was treated with Pt colloid and then exposed to CO and O₂ at 700 °C. The addition of Pt alters the response characteristics from p to n-type (compare with Fig. 4). The chemical state of Pt on the TiO₂ interface was investigated using XPS. Fig. 9a shows the XPS data for rutile-Pt in the Pt-4f region. The peak positions at 70.4 and 73.7 eV correspond to metallic Pt [23]. In addition to the metallic Pt, there is also significant contribution from PtO_x with a binding energy of 74.7 and 77.8 eV [35]. Fig. 9b shows the morphology of the rutile film with particles of 2 μm, and Fig. 9c is with the Pt colloids dispersed on the rutile thick film.

Fig. 10 shows the change of resistance of the Cr-doped rutile film with oxygen and CO at 800 °C. The resistance changes are similar to the rutile sample (Fig. 6), indicating p-type behavior towards O₂ and n-type towards CO.

4. Discussion

There is a striking difference in the resistance changes upon exposure of anatase and rutile films to O₂ and CO, as evidenced

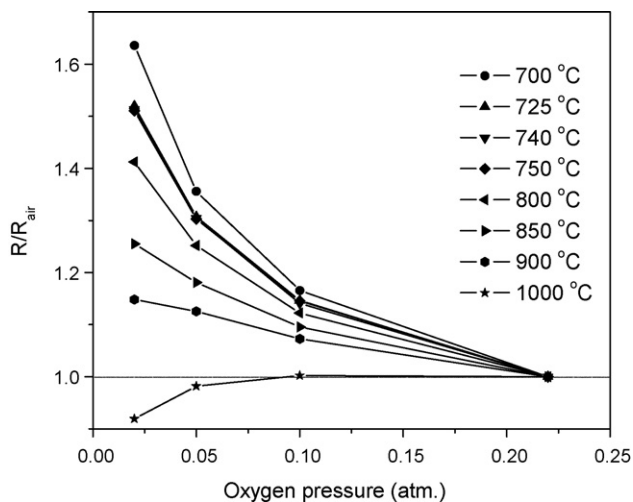
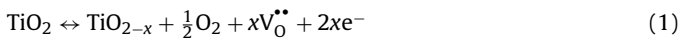


Fig. 7. Sensitivity of rutile film calcined at 1020 °C to oxygen at different temperatures.

from Figs. 3a and 4. The observations with the anatase film are consistent with earlier studies [9,27–31]. Upon heating the metal oxide, there is a loss of oxygen that leads to non-stoichiometry and n-type semiconducting property as shown by reaction (1),



where V_O depicts oxygen vacancy. Upon exposure to oxygen, chemisorbed oxygen species traps electrons at the surface (reaction (2), simplified representation as O_{ads}^-), thereby creating a barrier of electron flow between the anatase grains.



With increase in oxygen concentration, the resistance is expected to increase, as observed for the anatase films in Fig. 3a. The drop in resistance with increasing CO is readily understood from reaction (3):



causing an increase in the carrier (e^-) concentration and a decrease in the resistance. Minimal changes in resistance are observed for anatase films at temperatures exceeding 700 °C (Fig. 3b), and can be explained as arising from high concentration of electron carriers at the higher temperatures due to reaction (1) and therefore the

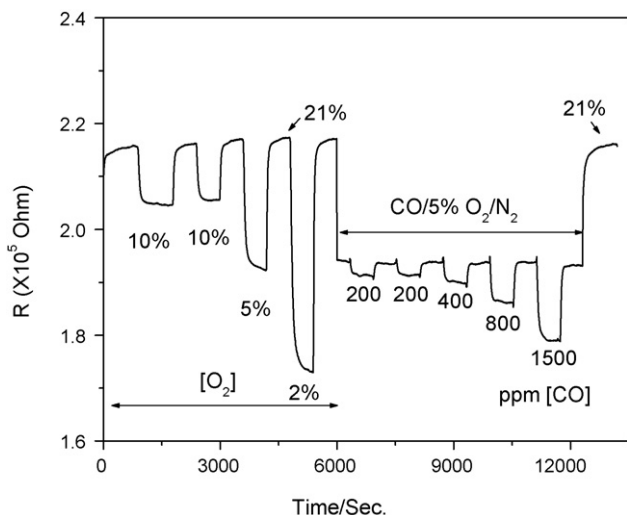


Fig. 8. Response of the Pt-rutile film to oxygen and CO at 700 °C.

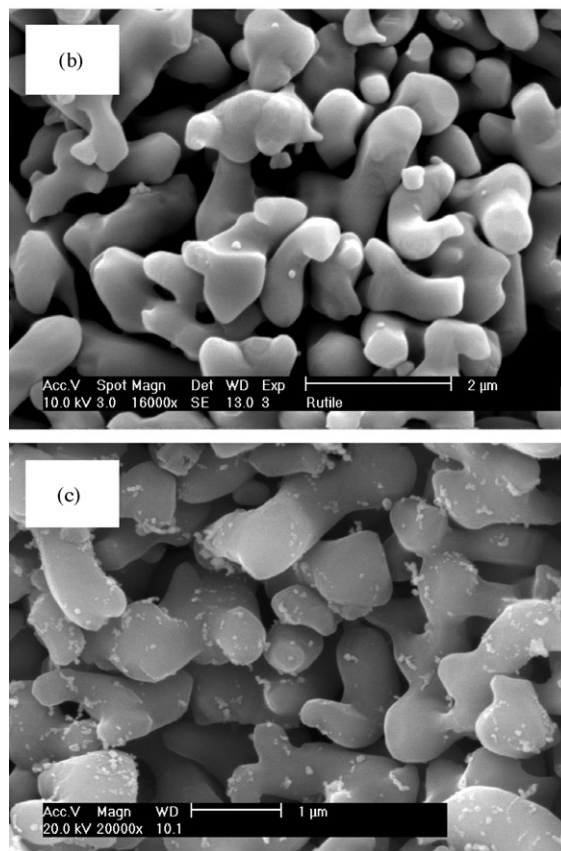
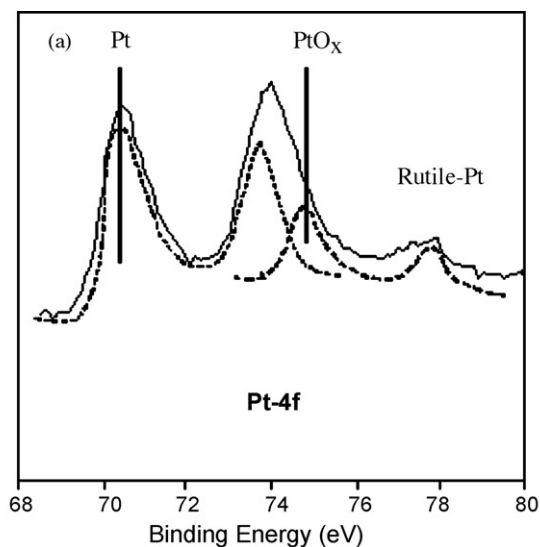


Fig. 9. (a) XPS spectra of Pt in 4f-region and surface morphology of (b) rutile and (c) Pt-rutile thick films.

relative changes of these carrier concentrations with CO reaction in the concentration range examined (reaction (3)) is minimal.

The following observations with the rutile sample are more complex and form the focus of this discussion:

Observation 1: p-type behavior towards oxygen (2–21%) at temperatures of 600–900 °C (Fig. 4).

Observation 2: Switch from p-type to n-type behavior between 10 and 5% O_2 at 1000 °C (Fig. 7).

Observation 3: p-type behavior to CO (200–1800 ppm) at background oxygen concentration of 2–10% O_2 at 600–725 °C (Fig. 4).

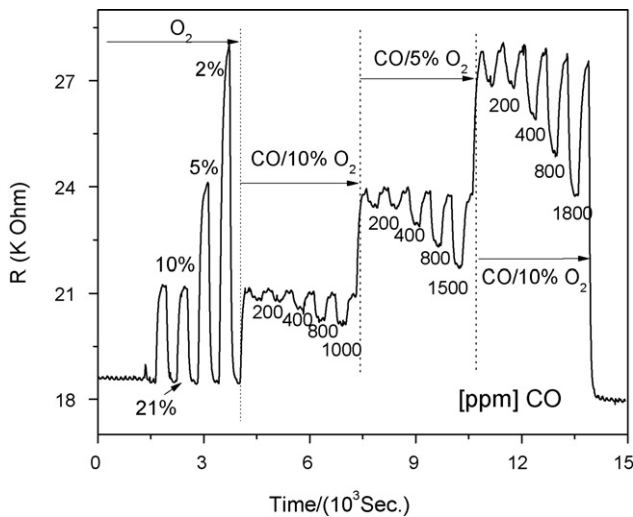


Fig. 10. Response of 0.5%Cr-doped rutile to oxygen and CO in different oxygen backgrounds at 800 °C.

Observation 4: Switch from p-type to n-type behavior with CO (0–200 ppm) at background oxygen concentration of 2–10% O₂ at and above 750 °C (Fig. 5).

Observation 5: Significant resistance changes with CO up to temperatures of 800 °C, and loss of response beyond this temperature (Fig. 6).

Observation 6: At a fixed concentration of O₂, requiring higher temperatures to switch from p to n-type for any concentration of CO (Fig. 5a).

Observation 7: At a fixed temperature (745 °C), requiring higher concentration of CO to make the p to n switch with increasing O₂ concentration.

It is important to point out that all electrical properties examined in this paper are based only on resistance, thus while we experimentally distinguish between n- and p-type behavior, we have not determined the majority charge carriers explicitly under the conditions of the experiment. With this caveat, we find that there are two models that can adequately describe these observations. However, indirect evidence does provide credence to one model, as we discuss below.

4.1. Model 1

Several studies have reported on the p-type behavior of polycrystalline rutile with O₂ in the temperature range of 700–1100 °C [2–6]. The explanation for p-type behavior is usually related to the presence of acceptor impurities. Impurities such as Al³⁺, Fe³⁺, Ca²⁺, can be incorporated into the lattice during the formation of rutile at high temperatures [2–6,9,32,36], as shown in reaction (4):



where A represents the impurity atom. The oxygen vacancies can be consumed by reaction with oxygen, thereby generating electron holes via reaction (5):



Thus, holes become the dominant charge carriers in rutile, leading to p-type conduction.

Using this model, we can explain the above observations as follows:

Observation 1: Since holes are the major carriers, O₂ adsorption increases number of holes via reaction (5) and so resistance decreases with increasing oxygen, as seen in Fig. 4.

Observation 2: As temperature increases, TiO₂ loses more oxygen releasing electrons (reaction (1)) and at 1000 °C and 5% O₂ the electrons become the majority carriers, as seen in Fig. 7.

Observation 3: There are two possible reactions with CO, reaction (3) above and reaction (6) with lattice oxygen (O_s):



Reaction (3) is expected at lower temperatures, whereas (6) is expected at higher temperatures. Both these reactions result in increase of electrons, which can then react with the majority holes resulting in an increase in the resistance as seen in Figs. 4 and 5a. Observation 4: As the CO concentration is increased above a certain limit at a particular temperature, the gas–solid interaction between CO and TiO₂ via reaction (6) can release electrons, overwhelming the holes as majority carriers, and exhibiting a n-type response, as seen in Fig. 6a.

Observation 5: The loss of response to CO at higher temperatures (>800 °C, Fig. 6b) is difficult to explain, since CO should continue to react with lattice oxygen.

Observation 6: At a fixed O₂ concentration, increasing temperature should lower oxygen adsorption, leading to reversal of reaction (5) and lower hole concentration. Thus, the p- to n-type transformation requires lower concentrations of CO.

Observation 7: At a fixed temperature with higher O₂ levels, reaction (5) is promoted, creating more holes and requiring higher concentration of CO via reaction (3) and/or (6) to revert to n-type behavior.

4.2. Model 2

This model considers, that, like anatase, rutile is also n-type with electrons as the majority carriers. However, strong oxygen adsorption on surface sites on rutile leads to formation of an inverted layer. The experimental observations can be explained as follows:

Observation 1: Oxygen adsorption leads to inversion so surface carriers are holes, and p-type behavior is observed.

Observation 2: Switch from p- to n-type at 5%O₂ is due to fewer O_{ads} (adsorbed oxygen) on the surface at the high temperature of 1000 °C and also because of increased oxygen vacancies (reaction (1)), which leads to increase in the electron concentration.

Observation 3: p-type behavior to CO since reaction of CO with O_{ads} decreases surface concentration of holes but the surface is still in the inverted state.

Observation 4: Decrease of inversion-causing O_{ads} at higher temperatures and further reaction of O_{ads} with CO leads to n-type behavior.

Observation 5: Above 800 °C, x in TiO_{2-x} is increased (reaction (1)), inversion effects are smaller and so CO reacting via reaction (3) does not alter the majority carrier concentration enough to make perceptible changes in resistance.

Observation 6: Requiring higher temperatures to switch from p- to n-type via reaction with CO at a fixed concentration of O₂ is because at higher temperatures, O_{ads} decreases minimizing the inversion effect and also electron concentration increases due to reaction (1).

Observation 7: Increasing concentration of oxygen increases O_{ads} increasing inversion, so requires higher concentration of CO to make the p to n switch.

Model 1 requires impurity cation insertion into TiO₂ lattice (reaction (4)) whereas Model 2 requires specific oxygen adsorption sites on the surface. In order to examine which of these models better represents the observations, further experiments were carried out. Doping of Cr³⁺ into the rutile structure was done by thermal

treatment. The strategy behind the Cr-rutile sample was based on the fact that Cr^{3+} with a radius of 0.615 Å can substitute for Ti^{4+} , which has a radius of 0.605 Å [32,36]. The substitution should promote p-type behavior (reaction (4)) and our goal was to examine if the Cr substitution would alter the properties towards O_2 and CO as compared to commercial rutile. However, as Fig. 10 shows, the behavior of Cr-doped rutile at 800 °C is very similar to rutile, with no evidence of p-type behavior towards CO.

The other experiment involved adding colloidal Pt to rutile. This led to conversion from p-type to n-type (Fig. 8). XPS analysis indicates the formation of PtO_x on the rutile surface (Fig. 9). Kirner et al. examined Pt diffusion in rutile at ~900 °C and based on XPS and Auger depth profiles concluded that Pt can diffuse into the subsurface layers of TiO_2 [35]. Since the solubility of Pt is negligible in TiO_2 , the interaction of Pt with the surface must be via interstitial positions as Pt^{m+} ($m=2, 3, 4$) within the top surface of the rutile particles. These defect sites can modify oxygen chemisorption. We propose that the presence of Pt on the rutile surface modifies the oxygen adsorption sites that cause inversion.

Thus, we are concluding that the profound differences between the anatase and rutile are related to differences in their surface structure which results in differences in oxygen chemisorption. Though we do not address the nature of these sites, it is known from the literature that anatase and rutile exhibit different properties. Anatase is a better photocatalyst than rutile [37]. Anatase is also of lower density than rutile and consists of distorted TiO_6 octahedrons [38]. Calculations suggest that the rutile surface (110) is easier to reduce as compared to anatase (101) [39].

The band bending that leads to inversion is controlled by surface adsorption effects. The surface states, typically within the energy gap of the semiconductor can arise from lattice imperfections and/or impurity atoms in the near-surface region. The XPS data in Fig. 2, especially for the O 1s region was carried out to discern if the surface oxygens were in any way different. Three peaks are observed, with the peak at 533.8 eV arising from adsorbed species that are not present in rutile due to the higher temperature treatment. The peak at 530.5 eV is unambiguous and assigned to O^{2-} of the TiO_2 framework. The peak at 531.5 eV has been assigned to oxygen bonded to Ti^{3+} , but we find no evidence of this oxidation state in the Ti2p XPS. Another assignment in the literature is to more covalent oxygen (O^-), arising from defect structures [34]. Both anatase and rutile exhibit the 531.5 eV peak, and we cannot use this information to infer about what surface sites in rutile are causing the inverted behavior. Another possibility is that transition metal impurities at the rutile surface are responsible for the strong binding to oxygen which results in inversion. The catalytic activity of CO to CO_2 oxidation is enhanced with Fe^{3+} -doped sample of rutile, and it has been proposed that Fe^{3+} substitutional doping on Ti^{4+} sites leads to generation of oxygen vacancies that can activate molecular oxygen by creation of superoxide and peroxide species [40]. The results with the chromium doped sample (Fig. 10) support this hypothesis. Also, the fact that the presence of the Pt on the surface reverts the rutile to n-type suggests that surface sites are relevant in these observations.

Inversion effects have been reported in the literature, though at significantly lower temperatures. Gurlo et al. observed n–p switching in $\alpha\text{-Fe}_2\text{O}_3$ at 280 °C with increasing O_2 concentration and with increasing CO at a fixed O_2 concentration [12,13]. They also measured the contact potential difference, which is an estimate of band bending and noted that the band bending increased as the switch from n- to p-type was observed.

In developing these models, we have assumed, based on the literature, that the contributions of ionic conductivity is negligible

at the temperatures and oxygen concentrations used in this study [41–43].

4.3. High temperature CO sensors

The peculiar properties of rutile surface provide an opportunity for using these films for CO sensing at temperatures as high as 800 °C, as shown in Fig. 6. To the best of our knowledge, such high temperatures for CO detection have been seldom reported in the literature. The only other high temperature CO sensing system that has been reported in the literature is based on Ga_2O_3 that performs at temperatures of 600 °C, and possibly higher [23–26]. The limitation of commonly used tin oxide or anatase for high temperature sensing is that in these materials, the sensing mechanism is controlled by grain boundary resistance. Intergranular resistance decreases with increase in majority carriers as a result of increased non-stoichiometry (x higher in TiO_{2-x}). Thus, at very high temperatures, the sensing response is controlled primarily by the oxygen defect chemistry and the intergranular contacts become irrelevant. This is the basis for rutile sensors for sensing O_2 at temperatures exceeding 1000 °C [6].

All metal oxides will exhibit this effect and oxygen sensors with Ga_2O_3 , SrTiO_3 , BaTiO_3 have been demonstrated [10,11]. However, these oxides that function based on oxygen defect equilibrium do not function well as reducing gas (e.g. CO) sensors because the change in oxygen partial pressure is typically too small at ppm (0–1000) levels of reducing gas.

With methane, sensing response is observed in the 750–800 °C range on Ga_2O_3 and it was proposed that the resistance changes are not controlled by grain boundaries, but rather by direct interaction of the gas with lattice oxygen, or by chemisorption of the reducing gas and injection of electrons into the solid [23–26]. Our hypothesis for the current rutile-based devices at 800 °C is that the resistance in background oxygen (2–21%) is controlled by p-type conductivity, and the switch to n-type upon CO introduction (200–1000 ppm) brings about a change in the majority carrier in the surface and results in a significant change in resistance. These data present a new paradigm for development of high temperature gas sensors for reducing gases.

5. Conclusions

The anatase thick film shows an n-type response, whereas, the rutile thick film exhibits p-type behavior for oxygen in the concentration range of 2–21% at temperatures below 1000 °C. However, with CO in the gas stream, depending on the CO and O_2 concentration and the temperature, both p-type and n-type behavior is observed. Incorporation of Cr^{3+} does not alter the properties of the rutile, but addition of platinum colloids on the surface of rutile results in n-type behavior. In anatase, oxygen non-stoichiometry is the main source of defect states, leading to n-type conduction behavior at elevated temperatures. On the other hand, in the case of rutile phase, there are two possibilities, impurity-induced oxygen vacancies lead to holes as the majority carriers or hole-based conduction can also result from inversion due to adsorption of oxygen on a n-type rutile surface. We conclude that the surface properties of the rutile are determining the resistance behavior and that the inversion model is more appropriate to explain the observations.

Acknowledgements

The authors would like to thank the Test Resource Management Center (TRMC) Test and Evaluation/Science and Technology (T&E/S&T) Program for their support. This work is funded by the

T&E/S&T Program through the Naval Undersea Warfare Center, Newport, RI, contract number N66604-07-C-1828.

References

- [1] P.I. Gouma, P.K. Dutta, M.J. Mills, Structural stability of titania thin films, *Nanestruct. Mater.* 11 (1999) 1231–1237.
- [2] U. Balachandran, N.G. Eror, Electrical conductivity in non-stoichiometric titanium dioxide at elevated temperatures, *J. Mater. Sci.* 23 (1988) 2676.
- [3] J. Nowotny, M. Radecka, M. Rekas, Semiconducting properties of undoped TiO₂, *J. Phys. Chem. Solids* 58 (1997) 927.
- [4] M. Radecka, M. Rekas, Effect of high temperature treatment on n–p transition in titania, *J. Am. Ceram. Soc.* 85 (2002) 346.
- [5] D.M. Smyth, The role of impurities in insulating metal oxides, *Prog. Solid State Chem.* 15 (1984) 145–171.
- [6] U. Kirner, K.D. Schierbaum, W. Gopel, B. Leibold, N. Nicoloso, W. Weppner, D. Fischer, W.F. Chu, Low and high temperature TiO₂ oxygen sensor, *Sens. Actuators B* 1 (1990) 103–107.
- [7] K. Zakrzewska, M. Radecka, M. Rekas, Effect of Nb, Cr, Sn additions on gas sensing properties of TiO₂ thin films, *Thin Solid Films* 310 (1997) 161.
- [8] T. Bak, J. Nowotny, M. Rekas, C.C. Sorrel, Defect chemistry and semiconducting properties of titanium dioxide. II. Defect diagrams, *J. Phys. Chem. Solids* 64 (2003) 1057.
- [9] N. Savage, S.A. Akbar, P.K. Dutta, Titanium dioxide based high temperature carbon monoxide selective sensor, *Sens. Actuators B* 72 (2001) 239–248.
- [10] J. Nowotny, M. Rekas, Electrical properties and defect structure of barium metatitanate within the p–type regime, *J. Eur. Ceram. Soc.* 5 (1989) 173.
- [11] W. Menesklou, H.-J. Schreiner, K.H. Härdtl, E.I. Tiffee, High temperature oxygen sensors based on doped SrTiO₃, *Sens. Actuators B* 59 (1999) 184.
- [12] A. Gurlo, M. Sahn, A. Oprea, N. Barsan, U. Weimar, A p- to n-transition on α -Fe₂O₃-based thick film sensors studied by conductance and work function change measurements, *Sens. Actuators B* 102 (2004) 291–298.
- [13] A. Gurlo, N. Barsan, A. Oprea, M. Sahn, T. Sahn, U. Weimar, An n- to p-type conductivity transition induced by oxygen adsorption on, *Appl. Phys. Lett.* 85 (12) (2004) 2280–2282.
- [14] J.L. Solis, V. Golovanov, V. Lantto, S. Leppävuori, S study of dual conductance response to carbon monoxide of CdS and α -SnWO₄ thin films, *Phys. Scripta T54* (1994) 248–251.
- [15] L.D. Birkefeld, A.M. Azad, S.A. Akbar, Carbon monoxide and hydrogen detection by anatase modification of titanium dioxide, *J. Am. Ceram. Soc.* 75 (11) (1992) 2964–2969.
- [16] K. Wiesner, H. Knözinger, M. Fleischer, H. Meixner, Working mechanism of an ethanol filter for selective high-temperature methane gas sensors, *IEEE Sens. J.* 2 (4) (2002) 354–358.
- [17] S.A. Akbar, P.K. Dutta, C. Lee, High-temperature ceramic gas sensors: a review, *Int. J. Appl. Ceram. Technol.* 3 (4) (2006) 302–311.
- [18] F. Ménil, V. Coillard, C. Lucat, Critical review of nitrogen monoxide sensors for exhaustive gases of lean burn engines, *Sens. Actuators B* 67 (2000) 1–23.
- [19] N. Miura, J. Wang, M. Nakatou, P. Elumalai, M. Hasei, NO_x sensing characteristics of mixed-potential-type zirconia sensor using NiO sensing electrode at high temperatures, *Electrochim. Solid State Lett.* 8 (2005) H9–H13.
- [20] T. Hibino, S. Wang, S. Kakimoto, M. Sano, Detection of propylene under oxidizing conditions using zirconia-based potentiometric sensor, *Sens. Actuators B* 50 (1998) 149–155.
- [21] J.W. Fergus, Solid electrolyte based sensors for the measurement of CO and hydrocarbon gases, *Sens. Actuators B* 122 (2) (2006) 683–693.
- [22] D. Koziej, K. Thomas, N. Barsan, F. Starzyk, U. Weimar, Influence of annealing temperature on the CO sensing mechanism for tin dioxide based sensors-Operando studies, *Catal. Today* 126 (2007) 211–218.
- [23] M. Fleischer, H. Meixner, Fast gas sensors based on metal oxides which are stable at high temperatures, *Sens. Actuators B* 43 (1997) 1–10.
- [24] A.C. Lang, M. Fleischer, H. Meixner, Surface modifications of Ga₂O₃ thin film sensors with Rh, Ru and Ir clusters, *Sens. Actuators B* 66 (2000) 80–84.
- [25] T. Schwebel, M. Fleischer, H. Meixner, C.-D. Kohl, CO-sensor for domestic use based on high temperature table Ga₂O₃ thin films, *Sens. Actuators B* 49 (1998) 46–51.
- [26] U. Hofer, J. Frank, M. Fleischer, High temperature Ga₂O₃-gas sensors and SnO₂-gas sensors: a comparison, *Sens. Actuators B* 78 (2001) 6–11.
- [27] P.K. Dutta, A. Ginwalla, B. Hogg, B.R. Patton, B. Chwieroth, Z. Liang, P. Gouma, M. Mills, S.A. Akbar, Interaction of CO with anatase surfaces at high temperatures: optimization of a CO sensor, *J. Phys. Chem. B* 103 (1999) 4412–4422.
- [28] N. Savage, B. Chwieroth, A. Ginwalla, B.R. Patton, S.A. Akbar, P.K. Dutta, Composite n–p semiconducting titanium oxides as gas sensors, *Sens. Actuators B* 79 (2001) 17–27.
- [29] P.K. Dutta, M.F. De Lucia, Correlation of catalytic activity and sensor response in TiO₂ high temperature gas sensors, *Sens. Actuators B: Chem.* 115 (2006) 1–3.
- [30] J. Trimboli, M. Mottern, H. Verweij, P.K. Dutta, Interaction of water with titania: implications for high-temperature gas sensing, *J. Phys. Chem. B* 110 (2006) 5647–5654.
- [31] J. Trimboli, P.K. Dutta, Oxidation chemistry and electrical activity of Pt on titania: development of a novel zeolite-filter hydrocarbon sensor, *Sens. Actuators B* 102 (2004) 132.
- [32] A.M. Venezia, L. Palmisano, M. Schiavello, Structural changes of titanium oxide induced by chromium addition as determined by an X-ray diffraction study, *J. Solid State Chem.* 114 (1995) 364–368.
- [33] J. Jun, M. Dhayal, J.-C. Kim, N. Getoff, Surface properties and photoactivity of TiO₂ treated with electron beam, *Radiat. Phys. Chem.* 75 (2006) 583–589.
- [34] J.-C. Dupin, D. Gonbeau, P. Vinatier, A. Levasseur, Systematic XPS studies of metal oxides, hydroxides and peroxides, *Phys. Chem. Chem. Phys.* 2 (2000) 1319–1324.
- [35] U.K. Kirner, K.D. Schierbaum, W. Göpel, Interface-reactions of Pt/TiO₂: comparative electrical, XPS-, and AES-depth profile investigations, *Fresen. J. Anal. Chem.* 341 (1991) 416.
- [36] J.-L. Carpentier, A. Lebrun, F. Perdu, Point defects and charge transport in pure and chromium-doped rutile at 1273 K, *J. Phys. Chem. Solids* 50 (2) (1989) 145–151.
- [37] P. Periyat, S.C. Pillai, D.E. McCormack, J. Colreavy, S.J. Hinder, Improved high-temperature stability and sun-light-driven photocatalytic activity of sulfur-doped anatase TiO₂, *J. Phys. Chem. C* 113 (2008) 7644–7652.
- [38] U. Diebold, Structure and properties of TiO₂ surfaces: a brief review, *Appl. Phys. A* 76 (2003) 681–687.
- [39] A. Bouzoubaa, A. Markovits, M. Calatayud, C. Minot, Comparison of the reduction of metal oxide surfaces: TiO₂-anatase, TiO₂-rutile and SnO₂-rutile, *Surface Sci.* 583 (2005) 107–117.
- [40] S. Carrettin, Y. Hao, V. Aguilar-Guerrero, B.C. Gates, S. Trasobares, J.J. Calvino, A. Corma, Increasing the number of oxygen vacancies on TiO₂ by doping with iron increases the activity of supported gold for CO oxidation, *Chem. Eur. J.* 13 (2007) 7771–7779.
- [41] D. Eder, R. Kramer, Electric impedance spectroscopy of titania: influence of gas treatment and of surface area, *J. Phys. Chem. B* 108 (2004) 14823–14829.
- [42] J. Nowotny, M. Radecka, M. Rekas, S. Sugihara, E.R. Vance, W. Weppner, Electronic and ionic conductivity of TiO₂ single crystal within the n–p transition range, *Ceram. Int.* 24 (1998) 571–577.
- [43] T. Anukunprasert, C. Saiwan, E. Di Bartolomeo, E. Traversa, Nanostructured TiO₂-based mixed metal oxides prepared using microemulsions for carbon monoxide detection, *J. Electroceram.* 18 (2007) 1295–1303.

Biographies

Xiaogan Li completed his undergraduate studies in China and received his Ph.D. from the Institute for Materials Research, Leeds University, U.K. He has just completed a postdoctoral fellowship at Ohio State University.

Ramamoorthy Ramasamy is currently working as a Powders Process Development Engineer at Diamond Innovations in Worthington, Ohio. His recent research interests are super-abrasive materials development, ceramic powders process design, high temperature gas sensor materials, and next generation composites development. Dr. Ramasamy received his Ph.D. in Physics from University of Madras, India and did his Post-Doctoral Research in the Ohio State University.

Prabir K. Dutta received his Ph.D. degree in Chemistry in 1978 from Princeton University. After 4 years of industrial research at Exxon Research and Engineering Company, he joined The Ohio State University, where currently he is Professor of Chemistry. His research interests are in the area of microporous materials and ceramics, including their synthesis, structural analysis, toxicity and as hosts for sensors, chemical and photochemical reactions.